THE ASTROPHYSICAL JOURNAL, 468:L13–L16, 1996 September 1

WFPC2 OBSERVATIONS OF THE COOLING FLOW ELLIPTICAL IN ABELL 1795[1]

JASON PINKNEY,[2] JON HOLTZMAN,[2] CHRISTOPHER GARASI,[2] ALAN M. WATSON,[2] JOHN S. GALLAGHER III,[4] GILDA E. BALLESTER,[5] CHRISTOPHER J. BURROWS,[6] STEFANO CASERTANO,[6] JOHN T. CLARKE,[5] DAVID CRISP,[7] ROBIN W. EVANS,[7] RICHARD E. GRIFFITHS,[8] J. JEFF HESTER,[9] JOHN G. HOESSEL,[4] JEREMY R. MOULD,[3] PAUL A. SCOWEN,[9] KARL R. STAPELFELDT,[7] JOHN T. TRAUGER,[7] AND JAMES A. WESTPHAL[10]

Received 1996 February 9; accepted 1996 June 19

ABSTRACT

We present WFPC2 images of the core of the cooling flow cD galaxy in Abell 1795. An irregular, asymmetric dust lane extends 7 h_{75}^{-1} kpc in projection to the north-northwest. The dust shares the morphology observed in the Hα and excess UV emission. We see both diffuse and knotty blue emission around the dust lane, especially at the ends. The dust and emission features lie on the edge of the radio lobes, suggesting star formation induced by the radio source or the deflection of the radio jets off of preexisting dust and gas. We measure an apparent R_V significantly less than 3.1, implying that the extinction law is not Galactic in the dust lane, or the presence of line emission that is proportional to the extinction. The dust mass is at least $2 \times 10^5\ h_{75}^{-2}\ M_\odot$ and is more likely to be $6.5 \times 10^5\ h_{75}^{-2}\ M_\odot$.

Subject headings: dust, extinction — galaxies: clusters: general — galaxies: elliptical and lenticular, cD

1. INTRODUCTION

Abell 1795 is a richness class 2 cluster and is one of the prototypical cooling flow clusters. Both X-ray spectral and surface brightness studies suggest an accretion rate of ~200 $h_{75}^{-2}\ M_\odot\ \mathrm{yr}^{-1}$ through a cooling radius of ~150 h_{75}^{-1} kpc. Like other cooling flow clusters, A1795 contains a cD galaxy at the peak of X-ray emission.

Optical observations of cooling-flow dominant galaxies (CFDs) reveal unusual phenomena possibly related to cooling flows (see reviews by Baum 1992 and Fabian 1994). Some contain nebulosity and filaments extending tens of kpc from the nucleus. The Hα + [N II] luminosities for CFDs are much higher than for noncooling flow ellipticals of equivalent radio power and correlate with mass accretion rate (Heckman et al. 1989). The emission line ratios suggest that both photoionized and shock-ionized gas may be present. McNamara & O'Connell (1992) find anomalous colors in the inner ≈20 kpc of CFDs; the bluest colors occur in the strongest cooling flows. There are also "blue lobes" of excess UV on top of the widespread blue light (McNamara & O'Connell 1993, hereafter MO93).

There is also evidence for dust in CFDs. NGC 1275 and 4696 have dust patches which are easily resolvable from the ground. Dust is inferred to be mixed with the emission-line gas from hydrogen recombination line ratios (Hu 1988), and from the absence of strong Ca II lines (Donahue & Voit 1993). About 50% of CFDs are detected in far IR, with luminosities suggesting larger dust masses than those inferred from optical observations (Bregman, McNamara, & O'Connell 1990). In Abell 1795, dust has not been clearly revealed in optical imaging (MO93). The presence of dust in CFDs is surprising because of the hot gas environment which should destroy dust on short timescales.

About 71% of CFDs contain radio sources which are generally amorphous or bipolar, and powerful (Burns 1990). They are confined to the inner ≈10 kpc of the CFD. This is also the realm of the emission line nebulosity and blue colors, so it has long been suggested that the radio source drives these phenomena (van Breugal, Heckman, & Miley 1984; MO93). The blue lobes (regions of UV excess) found in A1795, A2597, and NGC 1275 are observed to lie roughly on the edges of radio lobes (MO93; McNamara, O'Connell, & Sarazin 1995, hereafter MOS95). Hα and X-ray emission are also located along the edges of radio lobes (Cowie et al. 1983; MOS95). Photoionization of the Hα nebulae by an AGN is ruled out by inspecting the dependence of line ratios on distance from the AGN (Johnstone & Fabian 1988). Scattered light from the AGN is an unlikely cause of the blue lobes because the lobe light is not highly polarized (McNamara et al. 1996a). It appears more likely that hot, young stars produce the blue lobes (MOS95), and perhaps that star formation is being induced by the radio source (De Young 1995).

We present WFPC2 images of the center of the cD in A1795. The images clearly reveal a dust lane along with bluish filamentary and knotty emission features. There is a close correspondence between the radio source and the dust lane and emission features, and we discuss the nature of the radio/dust interaction. We also estimate the mass of the dust lane and compare the extinction law with the Galactic law.

[1] Based on observations with the NASA/ESA *Hubble Space Telescope*, obtained at the Space Telescope Science Institute, operated by AURA, Inc., under contract to NASA.

[2] Department of Astronomy, New Mexico State University, Dept. 4500, Box 30001, Las Cruces, NM 88003.

[3] Mount Stromlo and Siding Springs Observatories, Australian National University, Private Bag, Weston Creek Post Office, ACT 2611, Australia.

[4] Department of Astronomy, University of Wisconsin—Madison, 475 N. Charter Street, Madison, WI 53706.

[5] Department of Atmospheric, Oceanic, and Space Sciences, University of Michigan, 2455 Hayward, Ann Arbor, MI 48109.

[6] Astrophysics Division, Space Science Department, ESA and Space Telescope Science Institute, 3700 San Martin Drive, Baltimore, MD 21218.

[7] Jet Propulsion Laboratory, 4800 Oak Grove Drive, Pasadena, CA 91109.

[8] Department of Astronomy, Johns Hopkins University, 3400 N. Charles Street, Baltimore, MD 21218.

[9] Department of Physics and Astronomy, Arizona State University, Tyler Mall, Tempe, AZ 85287.

[10] Division of Geological and Planetary Sciences, California Institute of Technology, Pasadena, CA 91125.

2. THE DATA

An integration of 1780 s was obtained in each of the F555W and F702W filters using the Planetary Camera (PC) on 1994 February 24. We transformed the instrumental magnitudes into Johnson V and R, respectively, using the synthetic WFPC2 transformation given by Holtzman et al. (1995). Galactic reddening is negligible in the direction of A1795.

We combined our F702W and F555W images to create a color image (Fig. 1 [Pl. L3]). We subtracted an elliptical model from each image and averaged the results to produce Figure 2 (Plate L4). A dust lane appears dark in Figure 2 (labeled **D**) and as a dark, reddish feature in Figure 1. The absorption appears greatest near the nucleus, labeled **N**. We suspect the nucleus is the sharp peak seen at the same pixel in each filter, although dust may obscure the true nucleus. In the southernmost (**SKE**) and northernmost (**NKE**) extent of the dust lane, we see blue diffuse and knotty emission. Here, and in general around the periphery of the dust, we see the bluest knots, unresolvable in ground-based data. These may be star clusters, and are discussed in Holtzman et al. (1996). Some of these (**T**) are very elongated with the same position angle; two have unusual trails pointing NNW. Another notable feature is the southern linear filament (**SLF**) which appears to cross the cD just east of the nucleus. A northern filament (**NLF**) appears to be a faint continuation of the **SLF**. The faint Hα filaments (**FF**) in the SE corner are the end of a large filament observed to extend 45″ south of the nucleus (Cowie et al. 1983). In general, the image shows numerous clusters and bluish "stellar debris" (e.g., **SD**). In a separate Letter, McNamara et al. (1996b) suggest that the **NLF** and **SD** may be tidal debris from nearby ellipticals **E1** and **E2**.

The dust morphology is similar to the "irregular" and "asymmetric" dust seen in other *HST*-observed ellipticals (van Dokkum & Franx 1995). The dust is cospatial with an Hα feature (van Breugal, Heckman, & Miley 1984) and with the U-band excess (MO93). The U-band absorption feature in MO93 appears to have a different position than the dust in our image.

The majority of the galaxy, away from emission and absorption features, has $(V - R) \sim 0.5$–0.6. This is slightly bluer than most dominant ellipticals presented by Mackie, Visvanathan & Carter (1990). This entire inner region was found to be relatively blue in $(U - I)$ (MO93). The dust lane is red, with an average $(V - R) \sim 0.85$. The reddest region has $(V - R) = 1.4$ and is located within an unusual "cap" north of the nucleus (**N** in Fig. 2) which does not show strong dust absorption. The bluest regions occur in the **SLF** and have $V - R \sim 0.0$. Most of the **SLF** has $V - R \sim 0.4$, but there is a parallel red region running along the its west side (Fig. 1)—this filament may contain dust hidden under emission. When our $(V - R)$ map is smoothed to FWHM $\approx 1\farcs0$, it is apparent that the **SLF** is the bluest region in $(V - R)$. This is near the edge of the southern radio lobe and is coincident with one of the two blue lobes in MO93. The northern blue lobe in MO93 coincides with the dust lane and **NKE** (Fig. 2). It does not stand out in our smoothed color map because the blue knots are mixed with red dust.

3. COINCIDENCE WITH RADIO SOURCE

In Figure 3 (Plate L5), we overlay contours of 3.6 cm radio emission (Ge & Owen 1993). We assume that the radio core aligns with the apparent optical nucleus. We see a high degree of correspondence between the radio emission and optical features. The **SLF** shows its brightest knots where it meets the radio lobe (**SKE**). There appear to be parallel rows of emission and star formation in this filament (some inside of the radio emission), as if material was plowed by an advancing radio lobe. In general, the southern lobe appears bounded by the dark dust lane and the southern filament, the west side of which appears to be traced by dust (reddish in Fig. 1). Similarly, the northern radio lobe is nestled in the arc-shaped dust lane. Midway along the lane, the lobe appears to overlap the dust, but in general, the radio plasma appears bounded by the dust lane. A physical contact is supported by the sharper gradients in radio emission on the sides of the radio lobes which are next to the dust lane or filament. This is more apparent on the 6 cm map of van Breugal et al. (1984) which shows more extended emission on the east side of the northern lobe, and to the south and west of the southern lobe.

4. THE DUST LANE

The high resolution of these data allows us to map the absorption in A1795 with precision. We modeled the starlight of the underlying elliptical using ELLIPSE in IRAF.[11] To compensate for the presence of dust and excess emission, we excluded these regions from the fit; in F702W, we filled in excluded regions assuming reflection symmetry. The ellipse fitting was done by first fitting the outer 45–350 pixels (2″–15.″9) holding only the center fixed on the apparent nucleus, and then fitting the inner 45 pixels holding the center, position angle, and ellipticity fixed at values determined from the innermost annuli of the outer fit. If we fit for the center with the outer isophotes we get a location about 0.″3 south of the central peak, so the dust may be obscuring the nucleus. The quality of the fits was judged by plotting 3 pixel wide slices along three, apparently dust-free radial paths in the model-divided image. The photometric errors are ∼3%, and the model always matches within 10%.

We divided the data by the models to create extinction maps. The average extinction in 210 3×3 pixel regions is shown for both filters in Figure 4. The largest extinctions are 0.55 and 0.77 mag for A_{702} and A_{555}, respectively. The dashed lines outline the region that the extinctions can occupy for a physically thin sheet of dust obeying a Galactic extinction law (Cardelli, Clayton, & Mathis 1989). Our data appear outside of this region, obeying a linear relation for $A_{702} < 0.3$ given by $A_{555} = (1.62 \pm 0.05)\, A_{702} + 0.039 \pm 0.006$. The observed slope is greater than the maximum expected for Galactic extinction, 1.323, at the 5.9 σ level. The intercept is significantly different from 0.0, and is inconsistent with any extinction law.

We investigated possible systematic errors in our elliptical models which could reproduce our observations. Multiplicative errors in our models can only change the intercept. Our intercept is consistent with the F702W model being too small by 2.7%, or the F555W model being too large by 3.7%. Uniform additive errors can change both the intercept and the slope. An additive error of 0.6 DN in F702W can reproduce our intercept, but the slope is still ∼1.6 after this correction.

[11] IRAF is distributed by the National Optical Astronomy Observatories, which is operated by the Association of Universities for Research in Astronomy, Inc. (AURA), under cooperative agreement with the National Science Foundation.

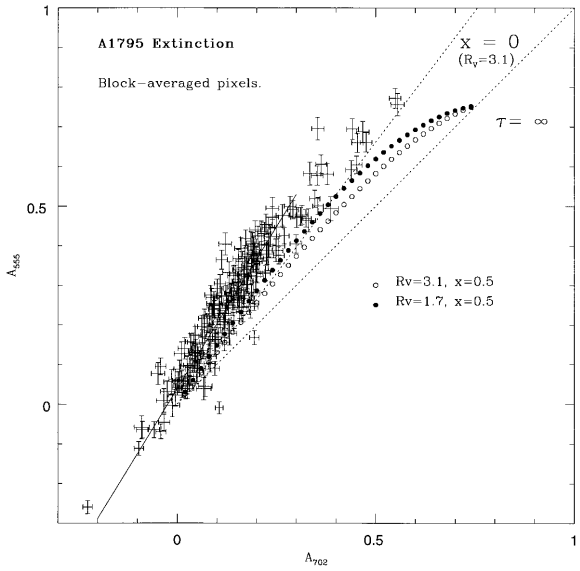

FIG. 4.—Average extinction in F555W and F702W filters for 210 3 × 3 pixel regions in the dust lane. The ordinate is extinction in the F555W band, and the abscissa is extinction in the F702W band. The solid line is a fit to points with $A_{702} < 0.3$. The dashed lines are the limits of extinction expected for a Galactic extinction law ($R_V = 3.1$). Lower limit: a dust sheet of infinite optical depth for varying depths into the galaxy. Upper limit: a dust screen positioned in front of all galaxy light (x, the fraction of light in front of the dust, = 0) with varying optical depth. The open circles trace out the extinction expected for $R_V = 3.1$ and $x = 0.5$. The filled circles are for $R_V = 1.7$ and $x = 0.5$.

To bring the slope to the Galactic value would require implausibly large additive errors.

Many natural phenomena make the apparent slope *less* than the true slope. Goudfrooij et al. (1994b, hereafter GDHN) show that foreground starlight, a homogeneous mixture of stars and dust, and scattered light all decrease the observed slope compared to the true extinction law. In fact, we see the influence of foreground light in Figure 4 as a "bending over" of the points at high extinctions, and we have attempted to compensate by fitting to low-extinction points only.

We find that both the apparent non-Galactic slope and nonzero intercept may be consequences of emission-line gas mixed with the dust. The Hα + [N II] map of A1795 (van Breugal et al. 1984) shows emission co-spatial with the dust which will decrease the apparent extinction in F702W and cause a positive intercept. However, if excess emission exists in the F555W band, it moves the intercept in the opposite sense and can cancel the F702W effect. We summed the equivalent widths of all emission lines in the "central nebula" using the data of Anton (1993) and find a *net contribution* of 4.0% to F702W. Thus, the excess emission in F702W is enough to produce the observed intercept.

The emission lines can also account for our non-Galactic slope if the emission is proportional to the extinction. Such a proportionality is observed in NGC 4696 (Sparks, Macchetto, & Golombek 1989, hereafter SMG), and is expected if the position of dust is correlated with that of gas. To produce the observed slope and intercept from an intrinsically Galactic extinction law, a total of 4031 DN in emission is required. The Hα + [N II] flux measured by van Breugal et al. (1984) in their regions marked "Nucleus" and "F3" sum to 18.6×10^{-15} erg cm^{-2} s^{-1}, which corresponds to 4378 DN, after an additional 60% has been added for other lines in F702W. Thus, it is likely that line emission that is correlated with the location of the dust is significantly affecting the observed slope and intercept in Figure 4. However, the van Breugal flux comes from an area larger than our dust region, so it is unclear whether there is really enough emission to produce the entire difference in slope. *HST* observations in line-free filters are required to clarify the true extinction law in the lane.

We estimated the dust mass by finding the average extinction in the dust lane region, excluding knots of emission, and converting it into V-band extinction using

$$A_V = A_\lambda \left[a(\lambda) + \frac{b(\lambda)}{R_V} \right], \quad (1)$$

where $a(\lambda)$ and $b(\lambda)$ are given in Cardelli et al. (1989), and the effective wavelengths for our filters are given by Holtzman et al. (1995). The gas mass was calculated using

$$N_{\rm H} = 5.8 \times 10^{21} \frac{A_V}{R_V} \text{ atoms cm}^{-2}, \quad (2)$$

which was found empirically by Bohlin et al. (1978), and then summing the number of atoms using the projected area of the region ($\approx 10\, h_{75}^{-2}$ kpc^2). We assume a gas/dust ratio of 100 and $R_V = 3.1$. This procedure gives a different dust mass for each filter: $M_{555} = 2.9 \times 10^5\ h_{75}^{-2}\ M_\odot$ and $M_{702} = 1.9 \times 10^5\ h_{75}^{-2}\ M_\odot$. These masses represent lower limits because of the presence of emission and foreground starlight, and possibly because of a non-Galactic extinction law. M_{555} is more accurate because the F555W band contains less line emission than F702W. It is likely that the dust is located near the center of the galaxy because the nuclear radio source appears to be interacting with the dust lane, and because our maximum extinction is about 0.75 mag. Compensating for the foreground light, we find $M_{555} = 6.5 \times 10^5\ M_\odot$. This is still a lower limit to the dust mass in A1795 because of line contamination in F555W, and because dust may be concealed in emission filaments (e.g., the **SLF**, Fig. 1) or in diffuse form.

5. DISCUSSION

5.1. *What Is the Origin of the Dust?*

The images clearly show dust in the A1795 CFD despite the harsh environment. The central temperature from X-ray spectra is 8.5×10^6 K (White et al. 1994), and a likely core gas density is ≈ 0.03 cm^{-3} (Ge & Owen 1993). Using these values, thermal sputtering is expected to remove refractory dust grains of radius 0.1 μm in only 6.7×10^6 yr (Draine & Salpeter 1979a). Since the lifetime is proportional to the grain radius, even if the dust were deposited 10^8 yr ago, all grains with radius $a \leq 1.5$ μm would already be destroyed. Clearly, the majority of the dust lane has been shielded from this hot gas environment. The extended low-ionization gas and recent star formation near the dust lane are evidence for a cocoon of gas with $T \ll 10^7$ K. This cocoon region may be the working surface of an "evaporation flow" (de Jong et al. 1990) where the hot ICM is ionizing gas and sputtering dust.

A complete sample of ellipticals from the RSA catalog has been studied by Goudfrooij et al. (1994a; GDHN). They detect dust in 41% and ionized gas in 57%. They argue for an external origin for the line + dust systems because the ionized gas is usually dynamically decoupled from the stellar velocity field and because internal mass loss cannot account for the quantity of dust. Their distribution of masses extends from $10^{3.2}\ M_\odot$ to $10^{6.3}\ M_\odot$ with an average near $10^{4.5}\ M_\odot$, so the dust mass in A1795 is relatively large. They measure apparent R_V-values that are, on average, lower than Galactic. They find

a tendency for regular dust morphologies (e.g., smooth rings, disks) to have the lowest R_V-values, and they conclude that both indicate highly evolved dust lanes. It is difficult to draw conclusions from the dust in A1795 because the R_V is still undetermined, and its irregular dust morphology may be caused by radio jet ram pressure rather than by accretion.

NGC 1275 (Perseus) and NGC 4696 (Centaurus) may provide better comparisons to the CFD in A1795. They are both centered in cooling flows and contain ionized gas, dust with irregular morphology, and powerful radio sources. The dust masses are also above average: NGC 1275 has $10^{6.3}$ $M_\odot$ (Goudfrooij et al. 1994a) and NGC 4696 has $10^{5.7}$ $M_\odot$ (GDHN; SMG). The extinction law appears to be indistinguishable from Galactic in these cases (SMG; GDHN; Nørgaard et al. 1993). Most of the dust in NGC 1275 is suspected to be a part of a system of ionized gas and recent star formation which has a systematically high velocity with respect to the nucleus (Nørgaard et al. 1993). The dust morphology of NGC 4696 is "half-spiral," like A1795, but does not appear to be interacting with its compact radio source (SMG). Thus, the best explanation for the dust in NGC 1275 and NGC 4696 is a recent galaxy merger. The fact that so many similarities exist between these three CFDs suggests a connection between the cooling flow phenomenon and mergers. One problem with this hypothesis is the expected rarity of mergers in rich cluster environments (e.g., Merritt 1985). Also, the CFD in A2029 contains no dust or ionized gas near its nucleus (McNamara & O'Connell 1992).

Although accretion from another galaxy is a likely origin of the dust lane, it is unlikely that all of the complexities of A1795 can be explained by one merger. In particular, the emission filaments are mostly blueshifted with respect to the center, they appear independent of the dust lane, and the line profiles near the central nebula show that two emission-line systems are present (Anton 1993). This is similar to NGC 1275, whose emission-line filaments appear to be independent of the merging, high-velocity system (Nørgaard et al. 1993). The widespread blue light (McNamara & O'Connell 1992) is also difficult to explain with a single, recent merger.

5.2. *What Is the Source of the Blue Lobes?*

Our data support the hypothesis that young stars are the source of the blue lobes in A1795. Apparent star clusters are now resolved at the positions of the lobes by these WFPC2 data. A comparison of our smoothed color map to our unsmoothed maps show that the bluest $(V - R)$ "lobe" occurs where star-cluster–like knots and diffuse emission are found. The northern blue lobe of MO93 is not apparent in smoothed $(V - R)$, but coincides with regions of dust embedded with bluish star clusters. Very young stars are required for the $U - I$ values, and so molecular gas may be present, probably with the dust lane and (dusty) linear filament which contain the lobes.

5.3. *What Role Does the Radio Source Play?*

We confirm that the blue lobes occur along the outer edge of the radio lobes of A1795. The knotty and diffuse bluish emission which appears to be the source of the U-band lobes is all located within 1 h_{75}^{-1} kpc of the radio lobes, in projection (Fig. 3). In general, bluish star clusters appear to be located preferentially near the lobes and jets. Thus, our data supports the enhancement of star formation by the radio source. However, the trailed clusters (**T**, Fig. 2) are bluish but appear in a region shielded from the radio source, so not all star formation is radio-induced. Lobe-induced star formation is feasible because of the heavy shocking expected at the lobe/IGM interface (Begelman & Cioffi 1989). The radio source may also provide the shock ionization of gas needed to explain spatial fluctuations in certain line ratios (e.g., [O III]/Hβ; Anton 1993).

We also see that dust is located on the outskirts of the radio lobes. It is ambiguous whether the radio jets have shaped the dust or vice versa, but an interaction is clear. This system should provide an interesting opportunity to study the interaction of radio jets with dusty media.

We thank B. McNamara for providing the digitized radio image. We are grateful to R. Walterbos, and J. O. Burns for engaging discussions. We utilized the NED Database and the ADS Abstract service for our research. This work was supported in part by NASA under contract NAS7-918 to JPL.

REFERENCES

Anton, K. 1993, A&A, 270, 60
Baum, S. 1992, in Cluster and Superclusters of Galaxies, ed. A. C. Fabian (Dordrecht: Kluwer), 171
Begelman, M. C., & Cioffi, D. F. 1989, ApJ, 345, 21
Bohlin, R. C., Savage, B. D., & Drake, J. F. 1978, ApJ, 224, 132
Bregman, J. N., McNamara, B. R., & O'Connell, R. W. 1990, ApJ, 351, 406
Burns, J. O. 1990, AJ, 99, 1
Cardelli, J. A., Clayton, G. C., & Mathis, J. S. 1989, ApJ, 345, 245
Cowie, L. L., Hu, E. M., Jenkins, E. B., & York, D. B. 1983, ApJ, 272, 29
De Jong, T., Nørgaard-Nielsen, H. U., Jørgensen, H. E., & Hansen, L. 1990, A&A, 232, 317
De Young, D. S. 1995, ApJ, 446, 521
Donahue, M., & Voit, G. M. 1993, 414, L17
Draine, B. T., & Salpeter, E. 1979, ApJ, 231, 77
Fabian, A. C. 1994, ARA&A, 32, 277
Ge, J. P., & Owen, F. N. 1993, AJ, 105, 778
Goudfrooij, P., Hansen, L., Jørgensen, H. E., & Nørgaard-Nielsen, H. U. 1994a, A&AS, 105, 341
Goudfrooij, P. de Jong, T., Hansen, L., & Nørgaard-Nielsen, H. U. 1994b, MNRAS, 271, 833 (GDHN)
Heckman, T. M., Baum, S. A., van Breugel, W. J. M., & McCarthy, P. 1989, ApJ, 338, 48
Holtzman, J. A., Burrows, C. J., Casertano, S., Hester, J. J., Trauger, J. T., Watson, A. M., & Worthey, G. 1995, PASP 107, 1065
Holtzman, J. A., Watson, A. M., Mould, J. R., Gallagher, J. S., & WFPC2 IDT. 1996, AJ, in press
Hu, E. M. 1988, in Cooling flows in Clusters and Galaxies, ed. A. C. Fabian (Dordrecht: Reidel), 73
Johnstone, R. M., & Fabian, A. C. 1988, MNRAS, 233, 581
Mackie, G., Visvanathan, N., & Carter, D. 1990, ApJS, 73, 637
McNamara, B. R., Jannuzi, B. T., Elston, R., Wise, M. W., & Sarazin, C. L. 1996a, ApJ, in press
McNamara, B. R., & O'Connell, R. W. 1992, ApJ, 393, 579
———. 1993, AJ, 105, 417 (MO93)
McNamara, B. R., O'Connell, R. W., & Sarazin, C. L. 1995, preprint (MOS95)
McNamara, B. R., Wise, M. W., Sarazin, C. L. Jannuzi, B. T., & Elston, R. 1996b, in press
Merritt, D. 1985, ApJ, 289, 18
Nørgaard, H. U., Goudfrooij, P., Jørgensen, H. E., & Hansen, L. 1993, A&A, 279, 61
Sparks, W. B., Macchetto, F., & Golombek, D. 1989, ApJ, 345, 153 (SMG)
van Breugal, W., Heckman, T., & Miley, G. 1984, ApJ, 276, 79
van Dokkum, P. G., & Franx, M. 1995, preprint
White, R. E. III, Day, C. S. R., Hatsukade, I., & Hughes, J. P. 1994, ApJ, 433, 583

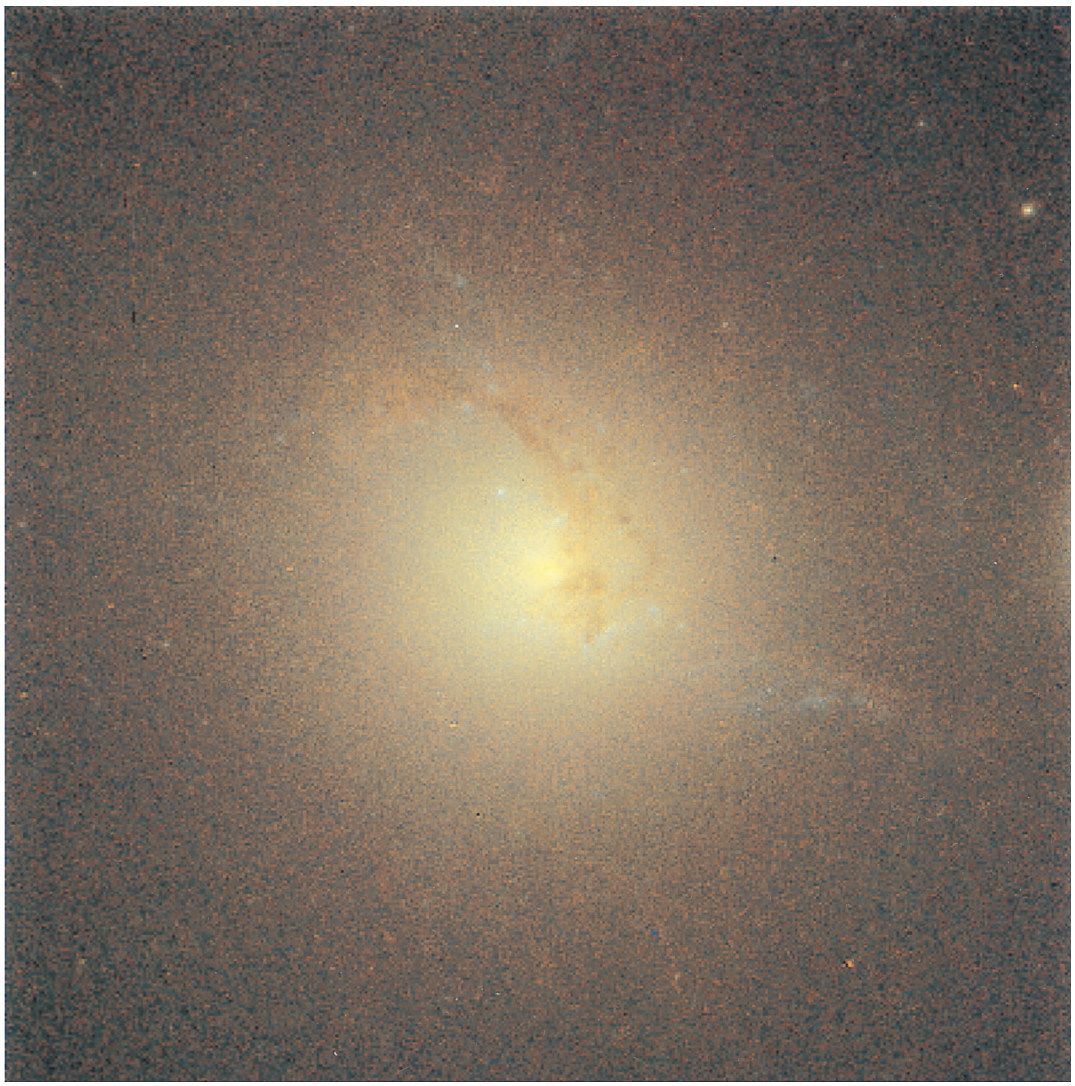

FIG. 1.—Color image of the CFD in A1795 created by assigning F702W to red, F555W to blue and a combination of the two to green. North is 55°CCW from up. The image is 18″ (20.2 h_{75}^{-1} kpc) on a side.

PLATE L4

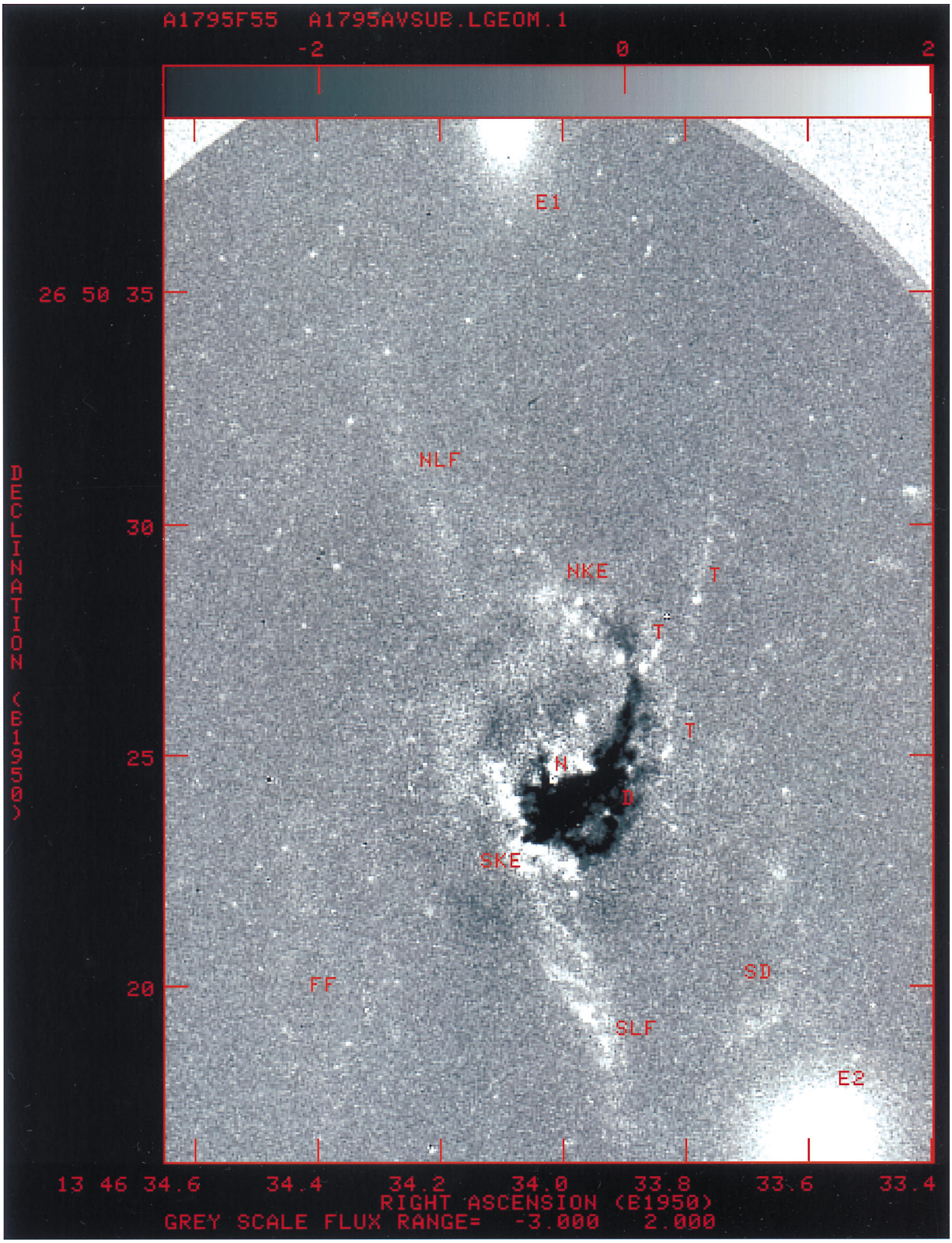

FIG. 2.—Image created by subtracting independent elliptical fits to the galaxy light from the F702W and F555W images and then averaging. The emission features (*light*) are emphasized with this technique. The absorption features (e.g., dust) appear dark. Labeled features are discussed in the text. North is to the top, and east is to the left.

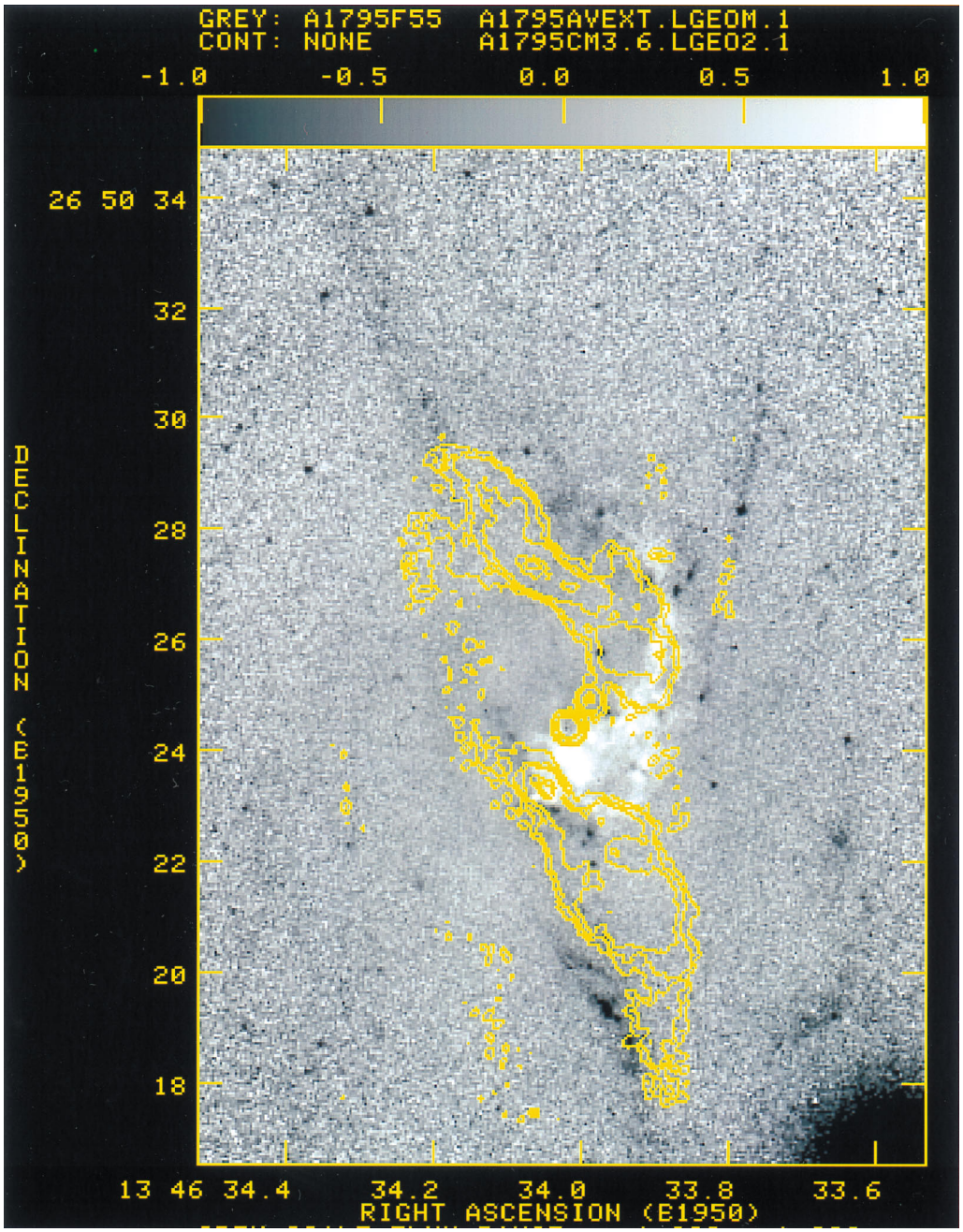

FIG. 3.—Overlay of 3.6 cm radio contours (scanned from Ge & Owen 1993) onto an extinction map gray scale. The extinction map was created by dividing the F702W and F555W images by elliptical models and then averaging to bring out faint features. North is to the top. Absorption features appear white.